analytical chemistry

Article

pubs.acs.org/ac

Mediatorless Glucose Biosensor and Direct Electron Transfer Type Glucose/Air Biofuel Cell Enabled with Carbon Nanodots

Mei Zhao, Yue Gao, Junyong Sun, and Feng Gao*

Laboratory of Functionalized Molecular Solids, Ministry of Education, Anhui Key Laboratory of Chemo/Biosensing, Laboratory of Optical Probes and Bioelectrocatalysis, College of Chemistry and Materials Science, Anhui Normal University, Wuhu 241000, People's Republic of China

Supporting Information

ABSTRACT: Utilization of carbon nanodots (CNDs), newcomers to the world of carbonaceous nanomaterials, in the electrochemistry realm has rarely been reported so far. In this study, CNDs were used as immobilization supports and electron carriers to promote direct electron transfer (DET) reactions of glucose oxidase (GOx) and bilirubin oxidase (BOD). At the CNDs electrode entrapped with GOx, a high rate constant (k_s) of 6.28 ± 0.05 s^{-1} for fast DET and an apparent Michaelis–Menten constant (K_M^{app}) as low as 0.85 ± 0.03 mM for affinity to glucose were found. By taking advantage of its excellent direct bioelectrocatalytic performances to glucose oxidation, a DET-based biosensor for glucose detection ranging from 0 to 0.64 mM with a high sensitivity of 6.1 μA mM^{-1} and a limit of detection (LOD) of 1.07 ± 0.03 μM (S/N = 3) was proposed. Additionally, the promoted DET of BOD immobilized on CNDs was also observed and effectively catalyzed the reduction of oxygen to water at the onset potential of +0.51 V (vs Ag/AgCl). On the basis of the facilitated DET of these two enzymes at CNDs electrodes, a mediator-free DET-type glucose/air enzymatic biofuel cell (BFC), in which CNDs electrodes entrapped with GOx and BOD were employed for oxidizing glucose at the bioanode and reducing oxygen at the biocathode, respectively, was successfully fabricated. The constructed BFC displayed an open-circuit voltage (OCV) as high as 0.93 V and a maximum power density of 40.8 μW cm^{-2} at 0.41 V. These important features of CNDs have implied to be promising materials for immobilizing enzymes and efficient platforms for elaborating bioelectrochemical devices such as biosensors and BFCs.

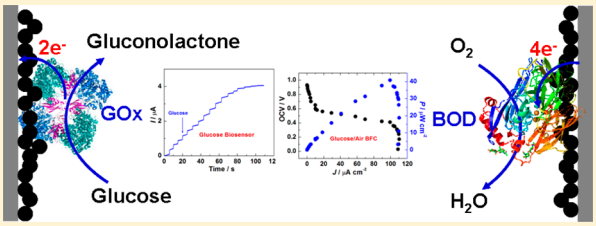

Achieving direct electron transfer (DET) between redox enzymes and electrodes is of great importance to fabricate advanced bioelectrochemical devices including biosensors, biofuel cells (BFCs), bioreactors, and other bioelectrocatalytic applications.[1−5] DET not only allows one to avoid the problems related to the utilization of extra reagents (redox mediators), such as limited stability, potential toxicity, and high cost,[4] but also offers relatively simple access for electrode architecture to miniaturize bioelectrochemical devices. Furthermore, the utilization near the redox-active site potential of the enzyme itself with a DET-based enzymatic electrode avails to improve power output of BFCs because the maximum cell voltage of BFCs is usually decreased by the use of redox mediators (for thermodynamic reasons). However, DET in enzymes generally occurs via redox metal centers or tunneling events,[4] and the efficient direct electrical communications between enzymes and electrodes are not common phenomena and often hampered by some obstacles.[6−10] These obstacles include unsuitable space orientation of enzymes to substrates, the proximity of active centers of enzymes beyond the electron-tunneling distance, denaturation of enzymes resulted from the adsorption,[6−9] and electrode passivation,[10] while enzyme molecules are immobilized on conventional bare electrodes.

Fortunately, chemically modified electrodes on which favorable functional materials, especially nanostructured materials, are modified could display electron-mediating functions and provide opportunities to facilitate the DET processes of redox enzymes and therefore have been considered as one of the most popular approaches.[11,12] Various structured nanomaterials composed of metal oxides[13−15] and conducting polymers[16,17] have appeared to facilitate DET reactions of enzymes, which may be attributed to the fact that the quantum-confined nanostructured materials could effectively reduce the electron-tunneling distance and thus play an electron-relaying role in DET.[13] To date, different carbon-based nanomaterials, including carbon nanotubes (CNTs), carbon nanofibers, carbon nanochips, and graphene oxide, have displayed the abilities to achieve DET of redox enzymes and shown to be ideal electrode materials for the DET-based bioelectrochemical applications, since they possess high electrical conductivity, good biocompatibility, ease of functionalization, and high surface-to-volume ratio.[18−38] However, significant challenges remain in the development of new nanomaterials which perform not only as an immobilization support for redox enzymes, but also as molecular wires to facilitate DET reactions for use in sensitive enzymatic sensors and BFCs with high energy conversion efficiency.

Received: July 25, 2014
Accepted: January 27, 2015
Published: January 27, 2015

DOI: 10.1021/acs.analchem.5b00012
Anal. Chem. 2015, 87, 2615−2622

Carbon nanodots (CNDs) are very interesting newcomers to the world of carbonaceous nanomaterials and constitute a fascinating class of nanocarbons which are comprise discrete, quasi-spherical nanoparticles.[39−43] Currently, the immense research interests in CNDs are primarily driven by their excellent photoluminescent properties and have shown their potential applications in a broad range of areas such as optical sensing, bioimaging, and light energy conversion.[39−41] Typically, comparing with other popular carbon-based nanomaterials including fullerenes, CNTs, and nanodiamonds, CNDs are easily available using different simple, fast, and cheap synthetic routes.[39−43] The discrete and quasi-spherical structures make CNDs also possess huge specific surface area and strong adsorption ability.[39] Furthermore, colloidal CNDs also display good biocompatibility, high electrical conductivity, and excellent chemical stability.[39−43] Obviously, it is reasonable to expect that CNDs can be suitable for biocatalysts supports and electrochemical signal transduction. However, little attention has been focused on the utilization of CNDs as supports for biological catalysts and signal transduction for electrochemistry by taking advantages of their remarkable properties and potential merits.[42,43]

Enzymatic electrochemical biosensors and BFCs are the areas where the efficient electrical contact between electrodes and enzymes is critical.[44−47] Glucose monitoring is an essential routine analysis in clinical medicine, especially for patients suffering from diabetes. In enzyme-based glucose biosensors, glucose oxidase (GOx) is one of the most widely utilized enzymes in glucose biosensors partly due to its high stability under normal conditions and its narrow substrate specificity toward glucose.[45−47] GOx, a structurally rigid dimeric glycoprotein containing two tightly bound flavin adenine dinucleotide (FAD) cofactors,[17] catalytically oxidizes glucose to gluconolactone with the aid of oxygen, accompanying the production of hydrogen peroxide and has been extensively used to fabricate enzymatic glucose biosensors via detecting the liberated H_2O_2 or consumed oxygen. However, both the electrooxidation of H_2O_2 and electroreduction of oxygen generally require high overpotential (i.e., a more positive potential for electrooxidation or a more negative potential for electroreduction) at conventional electrodes, which will severely affect the selectivity of the glucose biosensors because some electroactive species normally coexisted in the biological samples can also be oxidized or reduced at such potentials.[16] Therefore, in view of the distinguished advantages contributed from their natural simplicity and selectivity, DET-based glucose biosensors in which no mediators, even oxygen, are involved have attracted much extensive research efforts and innovation motivations. In several studies on DET of GOx, a pair of well-defined redox peaks originated from the active center (FAD/$FADH_2$) of GOx have been observed; however, the natural mediator, oxygen, is still needed to oxidize glucose, and therefore the mechanism for sensing glucose relies on detecting the increased oxidation currents from produced H_2O_2 or decreased reduction currents from consumed oxygen, instead of detecting the currents originated from direct oxidation of glucose.[14,15] Herein, a DET-type glucose biosensor without addition of any mediators has been reported, by immobilizing GOx on the CNDs-modified electrode.

On the other hand, BFCs, energy-converting devices from chemical energies to electrical energies in which enzymes rather than noble metals are employed as catalysts, have been envisaged as a novel type of clean, easily miniaturized, and implantable power source for powering biomedical electronic devices such as a cardiac pacemaker and insulin pump.[1,3,5,44,48−52] Glucose has been widely used as the fuel source in the construction of BFCs because glucose is ubiquitous and abundant in most living organisms.[4] The glucose-based BFCs developed to date have used either GOx[28,29] or glucose dehydrogenase (GDH)[21,24] as anodic biocatalyst to oxidize glucose, while bilirubin oxidase (BOD), laccase, and other blue copper oxidases have been utilized as cathodic biocatalysts to reduce oxygen.[26−38] The majority of the designed glucose/oxygen BFCs relied on the mediated electron transfer (MET) of GOx to fabricate the bioanodes.[44,45,53,54] Contrarily, few glucose/oxygen BFCs based on DET of GOx for direct bioelectrocatalytic oxidation of glucose have been developed.[26−31]

In this study, CNDs are considered as excellent immobilization matrixes and efficient electron carriers to facilitate DET of GOx and BOD, respectively. On the basis of the facilitated DET of these two enzymes at CNDs electrodes, a mediator-free third-generation glucose biosensor was fabricated via the direct bioelectrocatalysis of GOx to glucose oxidation, and furthermore, a DET-type glucose/air BFC was developed using GOx as anodic biocatalyst for glucose oxidation and BOD as cathodic biocatalyst for oxygen reduction, respectively. The performances and the potential applications of the proposed mediator-free glucose biosensor and DET-type glucose/air BFC were investigated, demonstrating that the constructed CNDs-based bioelectrodes have great potentials to elaborate bioelectrochemical devices such as biosensors and BFCs.

EXPERIMENTAL SECTION

Materials and Chemicals. Glucose oxidase (GOx, EC 1.1.3.4, 191 U mg^{-1}, from *Aspergillus niger*), and bilirubin oxidase (BOD, E.C.1.3.3.5, from *Myrothecium verrucaria*) were purchased from Fluka and used as received. β-D(+)-Glucose and Nafion perfluorinated ion-exchange resin (5 wt % solution in 90% light alcohol) were obtained from Sigma. All other chemicals were obtained from Sinopharm Chemicals Co., Ltd. (Shanghai, China). The reagents employed in this study are of at least analytical purity and used as received. Prior to use, the stock solution of glucose was let to equilibrate isomers for more than 1 day at 4 °C. Unless stated otherwise, a 20 mM, pH 7.2 phosphate buffer was used as supporting electrolyte and extensively purged with high-purity nitrogen before experiments when necessary. Milli-Q water (>18.0 MΩ) was used for the preparation of solutions. CNDs were prepared with candle soot as starting material according to reported methods,[40−42] and the details are provided in Supporting Information.

Electrode Preparation. In this study, the glassy carbon disc electrodes (GC) with diameters of 3 mm (CHI, Shanghai) were used as substrate electrodes to prepare different modified electrodes. In the preparing process, Nafion solution (0.5%, w/w) was used as binder to spread on the electrode surface. CNDs-modified GC electrode (defined as CNDs/GC), GOx, BOD-modified CNDs/GC electrode (defined as GOx-CNDs/GC, BOD-CNDs/GC, respectively) were prepared using the commonly used drop-cast method, and the details are provided in Supporting Information.

Apparatus. A CHI760D model potentiostat (CHI, Shanghai) combining a conventional three-electrode system, in which a modified electrode, Ag/AgCl, and platinum wire were used as the working electrode, reference electrode, and counter electrode, respectively, was employed for electro-

DOI: 10.1021/acs.analchem.5b00012
Anal. Chem. 2015, 87, 2615−2622

chemical measurements. The electrochemical measurements were carried out at ambient temperature and repeated at least three times. An FT-IR 8400S spectrophotometer (Shimadu, Japan) was used for IR spectra using KBr pellet samples. Morphological measurements of CNDs were performed on an S-4800 field emission scanning electron microscopy (SEM) (Hitachi, Japan), Hitachi H-600 transmission electron microscopy (TEM) (Tokyo, Japan), and JEOL-2010F high-resolution TEM (HRTEM) (JEOL, Japan) with an acceleration voltage of 200 kV, respectively. A PerkinElmer 2000 model FT Raman spectrometer (PerkinElmer, U.S.A.) was used for Raman spectra characterization of CNDs.

RESULTS AND DISCUSSION

Physicochemical and Electrochemical Characterization of CNDs. Figure S1 (Supporting Information) displays the typical SEM (Supporting Information Figure S1, parts A and B) and TEM (Supporting Information Figure S1, parts C and D) images of the prepared products, respectively. As shown in Supporting Information Figure S1, parts A and B, the low- and high-magnification SEM images of the resulting products indicate that they consist of a large amount of nanodots. The corresponding low- and high-magnification TEM images (Supporting Information Figure S1, parts C and D) reveal that they are nearly uniform spherical nanostructures with the diameters ranging from 50 to 60 nm. The prepared CNDs are hydrophobic and insoluble in common solvents and mainly contain elemental carbon (elemental analysis: C 95.09%, H 1.55%, O (calcd) 3.36%). Two distinct bands at 1340 cm^{-1} (D-band) and 1587 cm^{-1} (G-band) are shown in the Raman spectra (Supporting Information, Figure S2). In this case, the D-band generally originates from the A_{1g} symmetry of disordered graphite and indicates surface defects (e.g., distributed edge planes) are present at the surface of CNDs,[55,56] and the G-band is attributed to a zone-center mode of E_{2g} symmetry of single-crystal graphite.[55,56]

Figure S3 (Supporting Information) shows the cyclic voltammograms (CVs) recorded at CNDs/GC (Supporting Information Figure S3, curve a) and bare GC electrode (Supporting Information Figure S3, curve b) in phosphate buffer saline containing 0.1 M KCl. From this figure, we can see that the background voltammetric responses at CNDs/GC electrode in the applied potential window are featureless, suggesting that the CNDs electrode is nearly polarizable electrode. The background charging current measured at +0.2 V was calculated to be 141.0 $\mu A\ cm^{-2}$ for CNDs/GC and 14.3 $\mu A\ cm^{-2}$ for bare GC electrode, respectively. Furthermore, no obvious changes in charging currents were observed during the continuous scanning in the applied potential range, suggesting that CNDs film is stable on the electrode surface. The double layer capacitances of CNDs/GC and bare GC electrodes were found to be 287.2 and 14.4 $\mu F\ cm^{-2}$, respectively, which were calculated from the slopes of the plots of currents against scan rates, as shown in Figure S4 (Supporting Information). The increased capacitance of CNDs/GC electrode is attributed to the higher specific electrochemically active area of CNDs film coated on the GC electrode. The electrochemical surface area of CNDs coated onto a GC electrode was determined to be 0.62 cm^2, which is greater than that of a bare GC electrode (0.28 cm^2), or single-walled carbon nanotubes (SWNTs) modified GC electrode (0.46 cm^2), determined with Randles–Sevcik plots (Figure S5, Supporting Information) under identical conditions.

GOx Immobilization and Characterization. FT-IR spectroscopy could provide the information on the conformation changes and secondary structure of polypeptide chains and thus is generally employed for probing the structural variations of the native and immobilized enzymes.[57,58] Typically, this information could be displayed by the shapes and locations of FT-IR bands of enzymes including amide I absorption band, which is located at 600–1700 cm^{-1} and attributed to C═O stretching vibrations of the peptide linkage, and amide II absorption band, which is located at 1500–1600 cm^{-1} and originated from the combination of N–H in-plane bending and C–N stretching of the peptide groups.[58] In this study, the structural features of GOx were investigated with FT-IR spectroscopy after it was entrapped into CNDs film. As shown in Figure S6 (Supporting Information), the native GOx molecules (Supporting Information Figure S6, curve a) display three distinct peaks located at 1657, 1543, and 1103 cm^{-1}, which correspond to the amide I absorption band, amide II absorption band, and the C–O bond stretching vibration of GOx, respectively.[17,58] After being adsorbed onto CNDs, the absorption bands (Supporting Information Figure S6, curve c) of the amide I (1650 cm^{-1}) and II (1545 cm^{-1}) were almost as same as those of native GOx (Supporting Information Figure S6, curve a). The slight shifts of amide I and II absorption bands may result from hydrophobic interactions between GOx and CNDs.[59] It is generally accepted that the vanishing of the amide II band is responsible for the unfolding and denaturation of the immobilized enzymes.[59] In this study, the existence of the amide II absorption band demonstrates that GOx molecules entrapped into CNDs film retained their near-native states, and the CNDs–Nafion composite film displays good biocompatibility and strong affinity to GOx.

Electrochemical impedance spectroscopy (EIS) demonstrates that the charge-transfer resistance of the GOx-CNDs/GC electrode is higher than that of the CNDs/GC electrode, but lower than that of the GOx/GC electrode, suggesting that the presence of CNDs in the film enhances the transfer of electrons and thus decreases the resistance of the GOx–Nafion film (Figure S7, Supporting Information).

DET of GOx Immobilized in CNDs Film. The DET behaviors of GOx at GOx-CNDs/GC electrode were investigated by cyclic voltammetry. Figure 1 shows the CVs of CNDs/GC (Figure 1, curve a), GOx/GC (Figure 1, curve b), and GOx-CNDs/GC (Figure 1, curve c) electrodes performed in N_2-saturated phosphate buffer with a scan rate

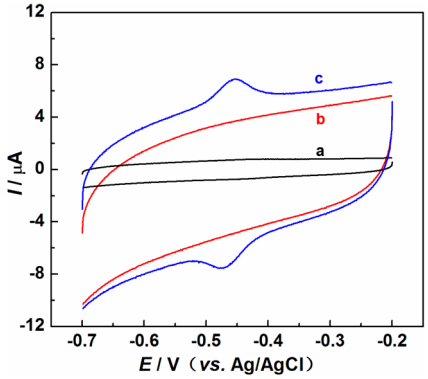

Figure 1. CVs obtained at CNDs/GC (a), GOx/GC (b), and GOx-CNDs/GC (c) electrodes in N_2-saturated phosphate buffer. Scan rate, 500 mV s^{-1}.

DOI: 10.1021/acs.analchem.5b00012
Anal. Chem. 2015, 87, 2615–2622

of 500 mV s^{-1}. As shown in this figure, a pair of distinct and almost symmetric redox peaks was observed at the GOx-CNDs/GC electrode (Figure 1, curve c), which could be originated from the electron transfer between GOx and the underlying electrode. We also can see from Figure 1 that the anodic peak potential (E_{pa}) and cathodic peak potential (E_{pc}) are −0.453 and −0.473 V (vs Ag/AgCl), respectively. The formal potential, $E^{0\prime}$, is −0.463 V, which is good agreement with previously published data for the FAD/$FADH_2$ redox center of GOx in a neutral solution.[13,14,17] Furthermore, the peak-to-peak separation, ΔE_p (defined as $\Delta E_p = E_{pa} - E_{pc}$), is ca. 20 mV and the ratio of anodic peak current (I_{pa}) and cathodic peak current (I_{pc}), I_{pa}/I_{pc}, was approximately 1, indicating that GOx immobilized in the CNDs−Nafion film displays a quasi-reversible redox electrochemical reaction. No obvious redox peaks were observed at the GOx/GC electrode (Figure 1, curve b), which is maybe resulted from the unreasonable orientation or denaturation of GOx molecules at substrate electrode, while GOx-CNDs/GC electrode could construct a biocompatible and conductive microenvironment which promotes DET between GOx and GC electrode with the aid of the entrapment of CNDs in the film. In order to achieve distinct voltammetric responses at the GOx-CNDs/GC electrode, the total mass loading and the mass ratios of GOx, Nafion, and CNDs in GOx-CNDs−Nafion composite system were optimized in control experiments (data not shown). The experimental results demonstrated that a total loading of ca. 4.6 μg and the mass ratios (in micrograms) for GOx, Nafion, and CNDs in GOx-CNDs−Nafion composite film of 2.0, 1.0, and 1.6, respectively, are optimal.

After several continuous CV cycles in buffer, the redox peak currents of GOx-CNDs/GC electrode arrived at steady state. In this study, all CV experiments at GOx-CNDs/GC electrode were performed at their steady states. The CVs of GOx-CNDs/GC electrode in deoxygenated buffer with different scan rates from 10 to 600 mV s^{-1} were collected. As shown in Figure S8A (Supporting Information), when increasing scan rates, E_{pa} and E_{pc} did not display obvious changes; at the meantime, the currents resulting from the DET of GOx were proportional to the increase of scan rates (Supporting Information Figure S8B), indicating that all electroactive GOx-FAD in the composite film is electroreduced to GOx-$FADH_2$ in the forward scan and then reoxidized to GOx-FAD in the backward scan. Substantially, the consumed charges (Q, coulombs), which could be calculated by integrating the area of anodic or cathodic peak in the CVs with subtracted background, were constant. And also, the cathodic current, I_{pc}, and anodic current, I_{pa}, were linearly dependent on scan rate, ν, and the slope ratio (S_{Ipc}/S_{Ipa}) from the $I_{pc}-\nu$ and $I_{pa}-\nu$ plots was close to 1 (Supporting Information Figure S8B). These results demonstrate that DET process of GOx immobilized in CNDs−Nafion film is a quasi-reversible and surface-controlled thin-layer electrochemical reaction.[14,17,59]

The average surface concentration of electroactive GOx (Γ^*, mol cm^{-2}) can be evaluated by the charge integration, and the amount of electroactive GOx molecules in the GOx-CNDs−Nafion film was found to be 4.08×10^{-11} mol cm^{-2} by the integration of the reduction peak of the GOx-CNDs/GC electrode at 100 mV s^{-1}, which is almost as 2.8 times as the theoretical value for monolayer coverage (1.89×10^{-11} mol cm^{-2})[60] and also larger than that of GOx immobilized on gold nanoparticles (9.8×10^{-12} mol cm^{-2})[61] and CdS colloid (1.54×10^{-11} mol cm^{-2}).[62] This result suggests that a few layers of GOx immobilized in the GOx-CNDs−Nafion film take part in the DET reaction. The absolute surface concentration of GOx cast on the geometric area of the electrode was estimated to be 1.22×10^{-10} mol cm^{-2}. Thus, the percentage of electroactive GOx for DET was calculated to be 33.4%, which is 2 times as high as the value (16.8%) reported for GOx immobilized in Nafion/nanostructured TiO_2 film.[14] These results further confirm that the CNDs−Nafion composite material provides a favorable microenvironment for GOx molecules and they well retain their native structure, as demonstrated with FT-IR spectroscopy.

The interfacial electron-transfer rate constant (k_s) at GOx-CNDs/GC electrode can be derived by the Laviron equation for diffusionless CVs when the potential separation of redox peak is less than 200 mV.[63] In this study, the k_s value was calculated to be 6.28 ± 0.05 s^{-1}, which is larger than the value of 3.96 s^{-1} for porous TiO_2,[14] 1.53 s^{-1} for multiwalled carbon nanotubes (MWNTs)-modified electrode,[64] and 0.3 s^{-1} for SWNTs-modified electrode,[65] revealing that the DET rate of immobilized GOx in CNDs−Nafion film is fast.

The influence of pH on the electrochemical behavior of the GOx-CNDs/GC electrode was also studied. Figure S9A (Supporting Information) displays the CVs at GOx-CNDs/GC electrode in electrolytic solution with various pH values ranging from pH 5.0 to 9.0, and it can be seen that the redox potential of the GOx is pH-dependent. The slope for $E^{0\prime}$−pH plot (Supporting Information Figure S9B) was estimated to be about −42.1 mV/pH, which is near the theoretical value for two-proton transfer coupled two-electron transfer reaction with the Nernst equation at 25 °C,[66] and well agrees with previously reported data.[13−17,59] This suggests that the proton diffusion in DET reaction of GOx is fast, and two protons ($2H^+$) and two electrons ($2e^-$) are involved in this DET reaction.

The direct bioelectrocatalytic activity of immobilized GOx to the oxidation of glucose was investigated and characterized by CVs at the GOx-CNDs/GC electrode in deoxygenated phosphate buffer with a scan rate of 100 mV s^{-1}. As depicted in Figure 2, without the addition of glucose to solution, a pair of well-defined and quasi-reversible redox peaks that originated from the reversible reaction of FAD/$FADH_2$ is observed. Once there was addition of glucose, the shape of the CVs at GOx-CNDs/GC electrode distinctly changed and an obvious increasing in the oxidation peak current was found; at the meantime, the reduction peak current was decreased. We also can see from this figure that the more amount of glucose was added, the greater the oxidation current was increased and the

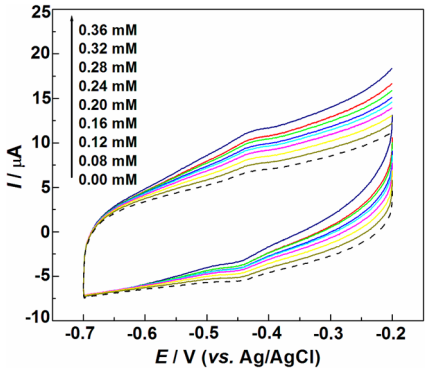

Figure 2. CVs of the GOx-CNDs/GC electrodes in N_2-saturated phosphate buffer containing different concentrations of glucose. Scan rate, 100 mV s^{-1}.

DOI: 10.1021/acs.analchem.5b00012
Anal. Chem. 2015, 87, 2615−2622

greater the reduction current was decreased. However, no corresponding electrochemical signals from the control results were found at CNDs/GC and GOx/GC electrodes, indicating that the catalytic process is resulted from the specific GOx-catalyzed reaction and that glucose oxidation at GOx-CNDs/GC electrode is based on DET. These results further demonstrate that the immobilized GOx molecules are bioactive and still maintain their natural biocatalytic activities toward their substrate, glucose, indicating that the CNDs electrode entrapped with GOx can be fabricated to be a glucose sensor or a bioanode to oxidize glucose in glucose-based BFC. The electrocatalytic processes could be explained that GOx-$FADH_2$ produced at the enzymatic electrode was first reduced by glucose, and subsequently, the obtained GOx-$FADH_2$ was reoxidized in cyclic catalytic reaction. When increasing the glucose concentration, more and more GOx-$FADH_2$ was chemically oxidized, leading to the increasing of GOx-$FADH_2$ oxidation peak and the decreasing of the GOx-FAD reduction peak. This result suggests that DET of GOx obtained at CNDs electrode can be effectively used for sensing glucose with no mediators involved. Obviously, the present sensing system is not only totally different from those of the first-generation glucose sensors, in which oxygen is needed and glucose detection relies on oxygen reduction in the presence of GOx, but also different from those of the second-generation glucose sensors, in which a redox relay is required to shuttle electrons between enzyme and electrode.[16,17]

To further investigate competitive reactions of oxygen reduction and glucose oxidation via DET of GOx, CV measurements of the GOx-CNDs/GC electrode were also conducted in air-saturated solution with various concentrations of glucose (Figure S10, Supporting Information). Different from the CVs obtained in N_2-saturated solution, a large cathodic current is found at GOx-CNDs/GC electrode in air-saturated solutions without glucose. However, the control experiments performed at CNDs/GC electrode do not show distinct cathodic current, apparently indicating that the large cathodic current observed at GOx-CNDs/GC electrode is attributed to oxygen reduction which is electrochemically catalyzed by the reduced GOx ($FADH_2$). When various concentrations of glucose were added into the air-saturated solution, the reduction peak currents are dependent on glucose concentrations and linearly decrease with the increasing of glucose concentration because the more glucose was added, the more oxygen was consumed for the enzymatic reaction between GOx and glucose. On the basis of the decreased electrocatalytic currents from the reduction of dissolved oxygen, this electrocatalytic system can also be employed to sense glucose in biological system containing oxygen.

Mediatorless Glucose Biosensor. Figure 3 displays the chronoamperometric $i-t$ response of GOx-CNDs/GC electrode to glucose poised at −0.463 V in a continuously stirring N_2-saturated buffer solution. As shown in this figure, the electrode responded rapidly to the substrate, glucose, when glucose was added into the solution. The oxidation current increased rapidly within about 3 s and then arrived at a stable current, reflecting the fast response of the present DET-based glucose biosensor to glucose. As shown in Figure 3 (inset, left panel), the oxidation currents display linear dependence on the glucose concentrations between 0 to 0.64 mM with a linear correlation coefficient (R) of 0.9984 (n = 16). The limit of detection (LOD) for glucose detection was calculated to be 1.07 ± 0.03 μM (S/N = 3), and a sensitivity for this DET-based

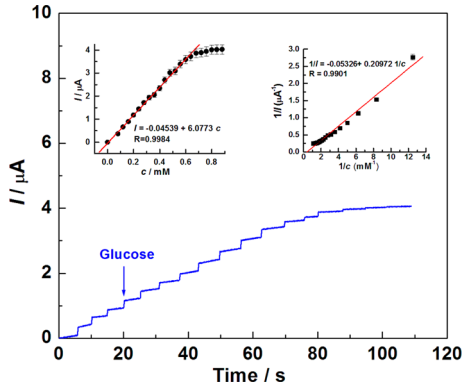

Figure 3. Chronoamperometric $i-t$ response of the GOx-CNDs/GC electrode to glucose with various concentrations in N_2-saturated phosphate buffer at −0.463 V. Inset: the corresponding calibration plot (current vs concentration, left panel) and the plot of $1/I_{ss}$ against $1/c$ (current^{-1} vs concentration^{-1}, right panel).

GOx electrode was found to be as high as 6.1 μA mM^{-1}, which is greatly higher than 0.3 μA mM^{-1} for GOx-porous TiO_2 electrode.[14]

As shown in the inset (left panel) of Figure 3, when the amount of added glucose is increased to a certain concentration, a catalytic current plateau is discernible, displaying the well-known Michaelis−Menten kinetic mechanism for enzyme-catalyzed reactions.[67] The apparent Michaelis−Menten constant (K_M^{app}) can be derived on the basis of the Lineweaver−Burk equation in electrochemical format, $1/I_{ss} = 1/I_{max} + K_M^{app}/(I_{max}c)$,[67] where I_{ss}, I_{max}, and c are the steady-state catalytic current in the presence of glucose, the maximum current with saturated glucose, and the glucose concentration in solution, respectively. The plot of $1/I_{ss}$ against $1/c$ is illustrated in Figure 3 (inset, right panel), and the value for K_M^{app} was found to be as low as 0.85 ± 0.03 mM, which is much lower than the value of 8.5 mM for GOx immobilized on carbon nanohorns,[68] 8.46 mM for GOx immobilized on CNT,[69] and 6.08 mM for GOx immobilized on TiO_2.[70] The low K_M^{app} value suggests that GOx immobilized into the CNDs−Nafion film keeps its higher bioactivity and shows better bioaffinity to glucose.

The storage stability of the GOx-CNDs/GC electrode was studied by monitoring the variation in its current response to 0.2 mM glucose. After storing for 2 weeks at 4 °C in refrigerator, the current was decreased by about 3.2% in comparison with initial current. The operation stability of the GOx-CNDs/GC electrode was also studied based on the successive assay of 0.2 mM glucose for 11 times with one same electrode, and a satisfactory relative standard deviation (RSD) value of 3.1% for repeated measurements (n = 11) was observed. In this study, the reproducibility for different GOx-CNDs/GC electrodes was also checked. Five electrodes, which were made independently but with the same method used in this study, were employed for measuring their current responses to 0.2 mM glucose, respectively, and showed a satisfactory RSD value of 3.3%. We believe the stable immobilizing of GOx in CNDs−Nafion film may be responsible for the good stability and reproducibility of GOx-CNDs/GC bioelectrode.

The GOx-CNDs/GC electrode also exhibits excellent selectivity for glucose detection. The effect of some interfering substances including ascorbic acid (AA), uric acid (UA),

DOI: 10.1021/acs.analchem.5b00012
Anal. Chem. 2015, 87, 2615−2622

dopamine (DA), and 4-acetamidophenol (AP) on glucose determination was investigated. As depicted in Figure 4, in the

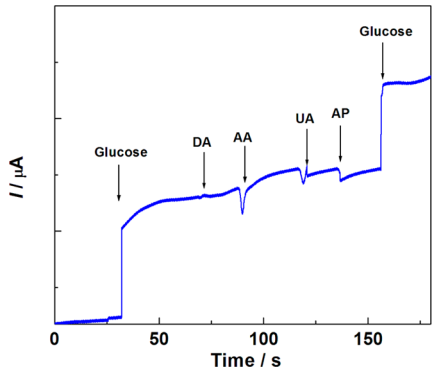

Figure 4. Amperogram response to 0.2 mM glucose at −0.463 V in the presence of different interfering substances including 0.2 mM DA, 0.3 mM AA, 0.5 mM UA, and 0.5 mM AP.

presence of interfering substances, including 0.3 mM AA, 0.2 mM DA, 0.5 mM UA, and 0.5 mM AP, the current for measuring 0.2 mM of glucose does not show obvious changes, whereas an obvious current response is observed again when 0.2 mM of glucose was subsequently introduced into the solution. These results demonstrate that the commonly existed interfering substances show little interference with glucose assay, indicating that the GOx-CNDs/GC electrode has potential application in real samples for glucose detection.

To further evaluate the applicability of the proposed glucose sensor, the present glucose biosensor was employed for the glucose detection in human serum. The sample treatments and measurements are shown in Supporting Information. As shown in Table S1 (Supporting Information), the results obtained with the proposed method show good agreements with the data provided by the hospital, indicating that the proposed glucose biosensor has great potential for detecting glucose in clinical samples.

DET-Type Glucose/Air BFC. As demonstrated above, direct bioelectrocatalytic oxidation of glucose near the redox-active potential of GOx can be successfully achieved at GOx-CNDs/GC electrode via DET reaction, making it desired for increasing the open circuit voltage (OCV) of the cell and suitable for a bioanode to construct a DET-type BFC. In this study, GOx-CNDs/GC enzymatic electrode was therefore used as the bioanode of glucose/air BFC.

BOD, one of blue copper oxidases, was selected for catalyzing the four-electron reduction of oxygen to water at the biocathode because BOD can efficiently work as an electrode biocatalyst even under neutral condition, while the optimum pH for most of the copper-containing oxidases (e.g., laccase) is in the slightly acidic region.[71,72] The DET of BOD at a variety of electrodes fabricated with carbon materials such as spectroscopic graphite, highly oriented pyrolytic graphite (HOPG), plastic-formed carbon, CNTs, carbon spheres, and porous carbonaceous has been reported.[23,25,26,73−76] In this study, the DET reaction of BOD on CNDs-modified film electrode was also investigated. Figure 5 displays the CVs recorded at BOD-CNDs/GC electrode in N_2 (Figure 5, curve a), air (Figure 5, curve b), or oxygen (Figure 5, curve c)-saturated phosphate buffer (pH 7.2). From Figure 5, we can see that the reduction currents are dependent on the concentration of the BOD substrate, oxygen. However, no reduction currents

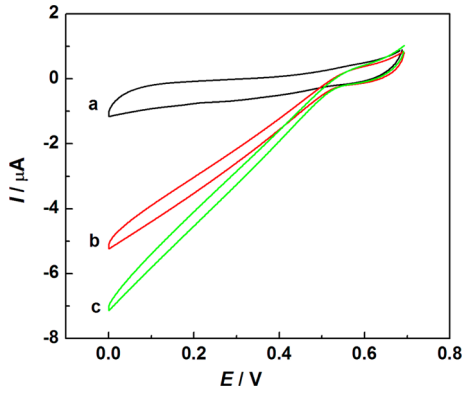

Figure 5. CVs of BOD-CNDs/GC electrode under nitrogen (a), air (b), or oxygen (c)-saturated phosphate buffer with a scan rate of 1 mV s^{-1}, respectively.

were observed at BOD/GC and CNDs/GC electrodes under the same experimental conditions, as shown in the control experiments (Figure S11, Supporting Information), suggesting that reduction currents observed at BOD-CNDs/GC electrode are resulted from BOD-catalyzed oxygen reduction and CNDs therefore promoted DET reaction of BOD. We also can see from Figure 5 that the catalytic current at BOD-CNDs/GC electrode commences at about +510 mV (vs Ag/AgCl), very approaching to the redox-active potential of the type I Cu site of BOD depicted in different literatures.[23,25,26,73−79] This result further demonstrates that DET of the BOD is successfully achieved at CNDs electrodes, suggesting that BOD-catalyzed O_2 reduction can be realized at a low overpotential. Such a novel BOD-based enzymatic bioelectrode is envisaged as the new biocathode of BFCs for oxygen reduction in neutral media.

Using GOx as a biocatalyst for direct bioelectrocatalytic oxidation of glucose, while BOD using as a biocatalyst for direct bioelectrocatalytic reduction of oxygen, a direct bioelectrocatalysis-based mediator-free glucose/air BFC (Scheme 1) was

Scheme 1. Illustration of the Fabricated DET-Type Glucose/Air BFC

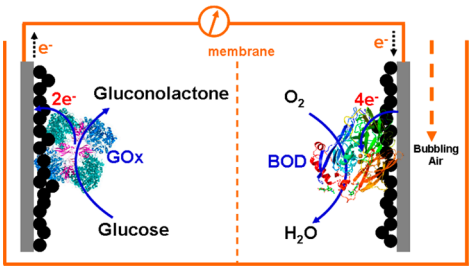

successfully developed. In this cell, dissolved O_2 intercepts the glucose oxidation-derived electrons from the bioanode, and it should react with the cathodic enzyme (BOD) and be reduced to water under normal circumstances.[31] As a result, electron flow from the bioanode to the biocathode is lower and power density will therefore be decreased compared to BFCs with two compartments separated by a membrane.[31] In this study, to hinder this phenomenon, a semipermeable membrane was used to separate the anode and cathode compartments.

Figure 6 shows two curves describing the dependence of both open circuit voltage (OCV, black dots) and power density (P, blue dots) on current density (j) of the fabricated CNDs-

DOI: 10.1021/acs.analchem.5b00012
Anal. Chem. 2015, 87, 2615−2622

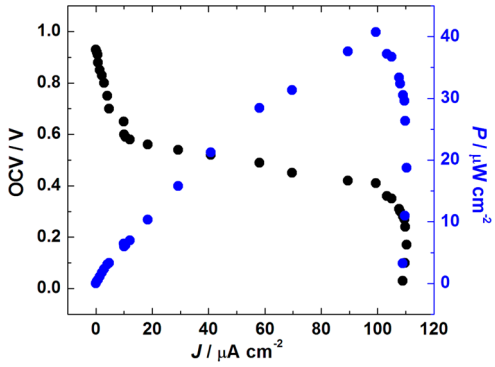

Figure 6. Polarization curve (black dots) and the dependence of power density of the assembled DET-based glucose/air BFC on current density (blue dots) in quiescent phosphate-buffered solution containing 4 mM glucose under air-saturated atmosphere.

based glucose/air BFC. As shown in this figure, the OCV for this BFC is as high as ca. 0.93 V and the density of power arrives at 40.8 μW cm^{-2} at 0.41 V. These performances of the present DET-type glucose/air BFC made with CNDs are quite comparable and even better than those provided in literatures for DET-type glucose/O_2 BFC (Table S2, Supporting Information). The stability of the present BFC was checked by measuring its power loss when it continuously worked in an air-saturated quiescent buffer containing 4 mM glucose coupling with 1 MΩ of resistance loaded on the cell. After operating for 24 h, the power of the BFC lost about 7.1%, and 37.4% after a duration of 7 days of continuous work. However, the OCV of the BFC remained unchanged during the duration.

CONCLUSIONS

A novel carbon material, CNDs, was synthesized, characterized, and used to immobilize GOx and BOD for DET reactions. The CNDs-based nanostructured electrode provides three-dimensional scaffolds for enzyme immobilization, within which enzymes themselves can act as three-dimensional conducting pathways and CNDs function as electron relays. The electrochemical behaviors of GOx and BOD immobilized on CNDs were investigated systematically. Taking advantage of the efficient DET-based bioelectrodes, a third-generation glucose sensor was built with a facile approach and displayed satisfactory sensing performances, and a DET-type glucose/air BFC was also fabricated combining GOx-CNDs/GC bioanode for directly oxidizing glucose and BOD-CNDs/GC biocathode for reducing oxygen. Conclusionally, the present studies demonstrate that CNDs can be envisaged as promising materials for entrapping enzymes and electrochemical transducer in biosensors and BFCs.

ASSOCIATED CONTENT

Supporting Information

Additional information that includes the preparations and characterization of CNDs and various modified electrodes, real sample measurements, and comparison results for different DET-type BFCs. This material is available free of charge via the Internet at http://pubs.acs.org.

AUTHOR INFORMATION

Corresponding Author

*Phone: +86-553-3937136. Fax: +86-553-3869302. E-mail: fgao@mail.ahnu.edu.cn.

Notes

The authors declare no competing financial interest.

ACKNOWLEDGMENTS

The funds from the Natural Science Foundation of China (no. 21175002), Program for New Century Excellent Talents in University (NCET-12-0599), Anhui Provincial Natural Science Foundation for Distinguished Youth (no. 1108085J09), and the project sponsored by SRF for ROCS, SEM, are acknowledged by all of the authors.

REFERENCES

(1) Nöll, T.; Nöll, G. *Chem. Soc. Rev.* **2011**, *40*, 3564−3576.
(2) Liu, Y.; Du, Y.; Li, C. M. *Electroanalysis* **2013**, *25*, 815−831.
(3) Osman, M. H.; Shah, A. A.; Walsh, F. C. *Biosens. Bioelectron.* **2011**, *26*, 3087−3102.
(4) Holland, J. T.; Lau, C.; Brozik, S.; Atanassov, P.; Banta, S. *J. Am. Chem. Soc.* **2011**, *133*, 19262−19265.
(5) Cooney, M. J.; Svoboda, V.; Lau, C.; Martin, G.; Minteer, S. D. *Energy Environ. Sci.* **2008**, *1*, 320−337.
(6) Léger, C.; Bertrand, P. *Chem. Rev.* **2008**, *108*, 2379−2438.
(7) Cracknell, J. A.; Vincent, K. A.; Armstrong, F. A. *Chem. Rev.* **2008**, *108*, 2439−2461.
(8) Gorton, L.; Lindgren, A.; Larrson, T.; Munteanu, F. D.; Ruzgas, T.; Gazaryan, I. *Anal. Chim. Acta* **1999**, *400*, 91−108.
(9) Rusling, J. F. *Acc. Chem. Res.* **1998**, *31*, 363−369.
(10) Stellwagen, E. *Nature* **1978**, *275*, 73−74.
(11) Ansari, S. A.; Husain, Q. *Biotechnol. Adv.* **2012**, *30*, 512−523.
(12) Chen, A.; Chatterjee, S. *Chem. Soc. Rev.* **2013**, *42*, 5425−5438.
(13) Si, P.; Ding, S.; Yuan, J.; Lou, X. W.; Kim, D. H. *ACS Nano* **2011**, *5*, 7617−7626.
(14) Bao, S. J.; Li, C. M.; Zang, J. F.; Cui, X. Q.; Qiao, Y.; Guo, J. *Adv. Funct. Mater.* **2008**, *18*, 591−599.
(15) Ivnitski, D.; Artyushkova, K.; Rincón, R. A.; Atanassov, P.; Luckarift, H. R.; Johnson, G. R. *Small* **2008**, *4*, 357−364.
(16) Wang, Z. Y.; Liu, S. N.; Wu, P.; Cai, C. X. *Anal. Chem.* **2009**, *81*, 1638−645.
(17) Guo, C. X.; Li, C. M. *Phys. Chem. Chem. Phys.* **2010**, *12*, 12153−12159.
(18) Armstrong, F. A.; Hill, H. A. O.; Oliver, B. N.; Walton, N. J. *J. Am. Chem. Soc.* **1984**, *106*, 921−923.
(19) George, S.; Lee, H. K. *J. Phys. Chem. B* **2009**, *113*, 15445−15454.
(20) Guiseppi-Elie, A.; Lei, C.; Baughman, R. H. *Nanotechnology* **2002**, *13*, 559−564.
(21) Yan, Y.; Zheng, W.; Su, L.; Mao, L. *Adv. Mater.* **2006**, *18*, 2639−2643.
(22) Shan, C. S.; Yang, H. F.; Song, J. F.; Han, D. X.; Ivaska, A.; Niu, L. *Anal. Chem.* **2009**, *81*, 2378−2382.
(23) Flexer, V.; Brun, N.; Courjean, O.; Backov, R.; Mano, N. *Energy Environ. Sci.* **2011**, *4*, 2097−2106.
(24) Gao, F.; Yan, Y.; Su, L.; Wang, L.; Mao, L. *Electrochem. Commun.* **2007**, *9*, 989−996.
(25) Tasca, F.; Gorton, L.; Harreither, W.; Haltrich, D.; Ludwig, R.; Nöll, G. *J. Phys. Chem. C* **2008**, *112*, 9956−9961.
(26) Gao, F.; Guo, X.; Yin, J.; Zhao, D.; Li, M.; Wang, L. *RSC Adv.* **2011**, *1*, 1301−1309.
(27) Coman, V.; Ludwig, R.; Harreither, W.; Haltrich, D.; Gorton, L.; Ruzgas, T.; Shleev, S. *Fuel Cells* **2010**, *10*, 9−16.
(28) Zebda, A.; Gondran, C.; Goff, A. L.; Holzinger, M.; Cinquin, P.; Cosnier, S. *Nat. Commun.* **2011**, *2*, 370 DOI: 10.1038/ncomms1365.
(29) Zebda, A.; Cosnier, S.; Alcaraz, J. P.; Holzinger, M.; Goff, A. L.; Gondran, C.; Boucher, F.; Giroud, F.; Gorgy, K.; Lamraoui, H.; Cinquin, P. *Sci. Rep.* **2013**, *3*, 1516 DOI: 10.1038/srep01516.
(30) Ramanavicius, A.; Kausaite, A.; Ramanaviciene, A. *Biosens. Bioelectron.* **2005**, *20*, 1962−1967.
(31) Min, K.; Ryu, J. H.; Yoo, Y. J. *Biotechnol. Bioprocess Eng.* **2010**, *15*, 371−375.

DOI: 10.1021/acs.analchem.5b00012
Anal. Chem. 2015, 87, 2615−2622

(32) Wang, S. C.; Yang, F.; Silva, M.; Zarow, A.; Wang, Y.; Iqbal, Z. *Electrochem. Commun.* **2009**, *11*, 34−37.
(33) Vincent, K. A.; Cracknell, J. A.; Lenz, O.; Zebger, I.; Friedrich, B.; Armstrong, F. A. *Proc. Natl. Acad. Sci. U. S. A.* **2005**, *102*, 16951−16954.
(34) Kamitaka, Y.; Tsujimura, S.; Setoyama, N.; Kajino, T.; Kano, K. *Phys. Chem. Chem. Phys.* **2007**, *9*, 1793−1801.
(35) Coman, V.; Vaz-Domínguez, C.; Ludwig, R.; Harreither, W. H.; Haltrich, D.; De Lacey, A. L.; Ruzgas, T.; Gorton, L.; Shleev, S. *Phys. Chem. Chem. Phys.* **2008**, *10*, 6093−6096.
(36) Murata, K.; Kajiya, K.; Nakamura, N.; Ohno, H. *Energy Environ. Sci.* **2009**, *2*, 1280−1285.
(37) Filip, J.; Šefčovičová, J.; Gemeiner, P.; Tkac, J. *Electrochim. Acta* **2013**, *87*, 366−374.
(38) Zhang, L.; Zhou, M.; Wen, D.; Bai, L.; Lou, B.; Dong, S. *Biosens. Bioelectron.* **2012**, *35*, 155−159.
(39) Baker, S. N.; Baker, G. A. *Angew. Chem., Int. Ed.* **2010**, *49*, 6726−6744.
(40) Li, H.; Zhai, J.; Sun, X. *Langmuir* **2011**, *27*, 4305−4308.
(41) Zhang, L.; Cui, P.; Zhang, B.; Gao, F. *Chem.—Eur. J.* **2013**, *19*, 9242−9250.
(42) Sheng, M.; Gao, Y.; Sun, J.; Gao, F. *Biosens. Bioelectron.* **2014**, *58*, 351−358.
(43) Dai, H.; Xu, G.; Gong, L.; Yang, C.; Lin, Y.; Tong, Y.; Chen, J.; Chen, G. *Electrochim. Acta* **2012**, *80*, 362−367.
(44) Calabrese Barton, S.; Gallaway, J.; Atanassov, P. *Chem. Rev.* **2004**, *104*, 4867−4886.
(45) Kavanagh, P.; Leech, D. *Phys. Chem. Chem. Phys.* **2013**, *15*, 4859−4869.
(46) Heller, A.; Feldman, B. *Chem. Rev.* **2008**, *108*, 2482−2505.
(47) Tremey, E.; Suraniti, E.; Courjean, O.; Gounel, S.; Stines-Chaumeil, C.; Louerat, F.; Mano, N. *Chem. Commun.* **2014**, *50*, 5912−5914.
(48) Yan, J.; Zhou, H.; Yu, P.; Su, L.; Mao, L. *Adv. Mater.* **2008**, *20*, 2899−2906.
(49) Halamkova, L.; Bocharova, V.; Alfonta, L.; Katz, E. *Energy Environ. Sci.* **2012**, *5*, 8891−8895.
(50) Willner, I.; Yan, Y. M.; Willner, B.; Tel-Vered, R. *Fuel Cells* **2009**, *9*, 7−24.
(51) Zhou, M.; Dong, S. *Acc. Chem. Res.* **2011**, *44*, 1232−1243.
(52) Falk, M.; Blum, Z.; Shleev, S. *Electrochim. Acta* **2012**, *82*, 191−202.
(53) Mano, N.; Mao, F.; Heller, A. *J. Am. Chem. Soc.* **2002**, *124*, 12962−12964.
(54) Gao, F.; Viry, L.; Maugey, M.; Poulin, P.; Mano, N. *Nat. Commun.* **2010**, *1*, 2 DOI: 10.1038/ncomms1000.
(55) McCreery, R. L. *Chem. Rev.* **2008**, *108*, 2646−2687.
(56) Katagiri, G.; Ishida, H.; Ishitani, A. *Carbon* **1988**, *26*, 565−571.
(57) Irace, G.; Bismuto, E.; Savy, F.; Colonna, G. *Arch. Biochem. Biophys.* **1986**, *244*, 459−469.
(58) Kauppinen, J. K.; Moffat, D. J.; Mantsch, H. H.; Cameron, D. G. *Appl. Spectrosc.* **1981**, *35*, 271−275.
(59) Wu, S.; Ju, H. X.; Liu, Y. *Adv. Funct. Mater.* **2007**, *17*, 585−592.
(60) Wang, S. F.; Chen, T.; Zhang, Z. L.; Shen, X. C.; Lu, Z. X.; Pang, D. W.; Wong, K. Y. *Langmuir* **2005**, *21*, 9260−9266.
(61) Liu, S. Q.; Ju, H. X. *Biosens. Bioelectron.* **2003**, *19*, 177−183.
(62) Huang, Y. X.; Zhang, W. J.; Xiao, H.; Li, G. X. *Biosens. Bioelectron.* **2005**, *21*, 817−821.
(63) Laviron, E. *J. Electroanal. Chem.* **1979**, *101*, 19−28.
(64) Cai, C. X.; Chen, J. *Anal. Biochem.* **2004**, *332*, 75−83.
(65) Liu, J. Q.; Chou, A.; Rahmat, W.; Paddon-Row, M. N.; Gooding, J. J. *Electroanalysis* **2005**, *17*, 38−46.
(66) Bard, A. J.; Faulkner, L. R. *Electrochemical Methods, Principle and Applications*, 2nd ed.; John Wiley & Sons, Inc: New York, 2001; pp 228−242.
(67) Lineweaver, H.; Burk, D. *J. Am. Chem. Soc.* **1934**, *56*, 658−666.
(68) Xu, G. B.; Liu, X. Q.; Shi, L. H.; Niu, W. X.; Li, H. J. *Biosens. Bioelectron.* **2008**, *23*, 1887−1890.
(69) Wang, Y. Y.; Wang, X. S.; Wu, B. Y.; Zhao, Z.; Yin, F.; Li, S.; Qin, X.; Chen, Q. *Sens. Actuators, B* **2008**, *130*, 809−815.
(70) Li, Q. W.; Luo, G. A.; Feng, J.; Zhou, Q.; Zhang, L.; Zhu, Y. F. *Electroanalysis* **2001**, *13*, 413−416.
(71) Mano, N.; Edembe, L. *Biosens. Bioelectron.* **2013**, *50*, 478−485.
(72) Solomon, E. I.; Sundaram, U. M.; Machonkin, T. E. *Chem. Rev.* **1996**, *96*, 2563−2605.
(73) Shleev, S.; Kasmi, A. E.; Ruzgas, T.; Gorton, L. *Electrochem. Commun.* **2004**, *6*, 934−939.
(74) Tsujimura, S.; Kano, K.; Ikeda, T. *J. Electroanal. Chem.* **2005**, *576*, 113−120.
(75) Tsujimura, S.; Kamitaka, Y.; Kano, K. *Fuel Cells* **2007**, *7*, 463−469.
(76) Ramírez, P.; Mano, N.; Andreu, R.; Ruzgas, T.; Heller, A.; Gorton, L.; Shleev, S. *Biochim. Biophys. Acta* **2008**, *1777*, 1364−1369.
(77) Tsujimura, S.; Kuriyama, A.; Fujieda, N.; Kano, K.; Ikeda, T. *Anal. Biochem.* **2005**, *337*, 325−331.
(78) Ramírez, P.; Mano, N.; Andreu, R.; Ruzgas, T.; Heller, A.; Gorton, L.; Shleev, S. *Biochim. Biophys. Acta* **2006**, *1757*, 1634−1641.
(79) Zheng, W.; Li, Q.; Su, L.; Yan, Y.; Zhang, J.; Mao, L. *Electroanalysis* **2006**, *18*, 587−594.

DOI: 10.1021/acs.analchem.5b00012
Anal. Chem. 2015, 87, 2615−2622